

RESEARCH PAPER

## Anticancer Activity of Zinc Oxide Nanoparticles Biosynthesized Using *Urtica pilulifera* L. Extract Against U87 Glioblastoma Cancer Cells

Jaafar Nashid Hameed<sup>1</sup>, Athraa Kareem Abas<sup>2</sup>, Muthik A. Guda<sup>1\*</sup>

<sup>1</sup> Department of Ecology, Faculty of Sciences, University of Kufa, Iraq

<sup>2</sup> Department of Biology, Faculty of Education for Girls, University of Kufa, Iraq

### ARTICLE INFO

#### Article History:

Received 20 March 2026

Accepted 11 May 2026

Published 01 July 2026

#### Keywords:

Apoptosis

Cytotoxicity

Glioblastoma

*Urtica pilulifera*

ZnO NPs

### ABSTRACT

The rapid expansion of green nanotechnology has driven renewed interest in environmentally safe approaches for producing biomedical nanomaterials. Among these, zinc oxide nanoparticles (ZnONPs) have attracted considerable attention due to their biocompatibility, chemical stability, and notable anticancer properties. Their nanoscale dimensions enhance cellular interactions and promote selective toxicity toward malignant cells, making them promising candidates for therapeutic development. In this study, ZnONPs were synthesized using an aqueous extract of *Urtica pilulifera* leaves as a natural reducing and stabilizing agent. Phytochemical screening confirmed the presence of flavonoids, phenolics, tannins, alkaloids, and terpenoids, all of which contributed to nanoparticle formation. The synthesized particles were characterized using FE-SEM to verify their optical, structural, and morphological features, UV-Vis spectroscopy, XRD, FTIR, and. Cytotoxic effects were evaluated against U87 glioblastoma cells using the MTT assay. Characterization revealed that the ZnONPs were spherical, crystalline, and coated with phytochemicals from the plant extract. Biological assays demonstrated a concentration-dependent reduction in U87 cell viability, accompanied by clear apoptotic indicators such as cell shrinkage and membrane disruption. The findings highlight the strong anticancer potential of green-synthesized ZnONPs, emphasizing their suitability as eco-friendly and effective agents for future applications in nanomedicine.

### How to cite this article

Hameed J., Abas A., Guda M. Anticancer Activity of Zinc Oxide Nanoparticles Biosynthesized Using *Urtica pilulifera* L. Extract Against U87 Glioblastoma Cancer Cells. J Nanostruct, 2026; 16(3):3190-3200. DOI: 10.22052/JNS.2026.03.015

### INTRODUCTION

Cancer remains a formidable global health challenge, characterized by aggressive cellular proliferation and metastatic potential, which often lead to poor clinical outcomes. The complexity of the tumor microenvironment and the innate ability of malignant cells to evade programmed

\* Corresponding Author Email: [meethakha.almithhachi@uokufa.edu.iq](mailto:meethakha.almithhachi@uokufa.edu.iq)

cell death (apoptosis) make it a leading cause of mortality worldwide [1]. Among the most lethal forms of malignancy is Glioblastoma Multiforme (GBM), represented by the U87 cell line, which is notorious for its rapid progression and resistance to standard interventions [2]. While conventional therapies such as chemotherapy and radiotherapy



This work is licensed under the Creative Commons Attribution 4.0 International License.

To view a copy of this license, visit <http://creativecommons.org/licenses/by/4.0/>.

are widely utilized, their clinical efficacy is frequently compromised by severe systemic toxicity, non-specific targeting of healthy tissues, and the rapid emergence of multi-drug resistance (MDR) [1, 2, 3]. These therapeutic hurdles underscore the urgent need for innovative, highly selective, and biocompatible anticancer agents that can deliver maximum lethality to tumor cells with minimal collateral damage to normal physiological systems [3].

In response to these challenges, recent biomedical research has pivoted toward nanotechnology to develop “smart” therapeutic modalities. Nanoparticles (NPs), due to their unique physicochemical properties including a high surface-area-to-volume ratio and enhanced cellular permeability offer a superior platform for targeted drug delivery and intrinsic cytotoxicity [4]. Among various inorganic nanomaterials, zinc oxide nanoparticles (ZnONPs) have gained significant prominence in oncology. ZnONPs are recognized for their inherent ability to induce selective apoptosis in malignant cells via the generation of reactive oxygen species (ROS), which triggers oxidative stress and mitochondrial dysfunction [4, 5]. Furthermore, their pH-sensitive nature allows for the accelerated release of Zn<sup>2+</sup> ions in the acidic microenvironment of tumors, further enhancing their selective toxicity while maintaining a favorable safety profile for healthy tissues [5].

Despite the therapeutic potential of ZnONPs, traditional synthesis routes involving physical and chemical methods often present significant environmental and biological drawbacks. These processes frequently utilize hazardous reducing agents, such as sodium borohydride, and require high energy consumption, leading to the production of toxic by-products [6]. To address these sustainability concerns, “green synthesis” has emerged as an eco-friendly and cost-effective alternative. This approach utilizes biological materials specifically plant extracts to serve as both reducing and stabilizing agents in a single-step reaction [6, 8]. Green-synthesized nanoparticles often exhibit superior biocompatibility and enhanced biological activity due to the natural “capping” of bioactive molecules on their surface, which prevents aggregation and improves stability [8].

In this context, *Urtica pilulifera* (Roman Nettle) represents an ideal biological scaffold for

nanoparticle fabrication. This medicinal plant is exceptionally rich in secondary metabolites, including phenolic acids, flavonoids, tannins, and terpenoids, which are known for their potent antioxidant and reducing capabilities [7]. These phytochemicals facilitate the efficient reduction of zinc precursors into stable nanoparticles while providing a natural layer of bioactive compounds that may synergistically enhance the anticancer effects [7, 8]. Although the general properties of ZnONPs are well-documented, the specific interaction between *U. pilulifera*-mediated nanoparticles and aggressive brain cancer models like U87 glioblastoma remains an area that requires comprehensive investigation to optimize dose-dependent responses and therapeutic outcomes.

This study aims to synthesize zinc oxide nanoparticles using an aqueous extract of *U. pilulifera* via a one-pot, eco-friendly green approach. Following synthesis, the physicochemical features of the produced ZnONPs including their morphology, crystallinity, and size distribution are characterized using advanced analytical instruments such as SEM, XRD, and UV-Vis spectroscopy. Finally, the research assesses the anticancer activity and dose-dependent effects of these synthesized ZnONPs against U87 glioblastoma cells *in vitro*. By exploring the cytotoxic thresholds and the induction of apoptosis in these resistant cells, this work seeks to provide new insights into the development of plant-mediated Nano medicines as a potent and selective tool for targeted cancer therapy.

## MATERIALS AND METHODS

### *Plant Collection and Extraction*

Fresh leaves of *U. pilulifera* were collected from uncontaminated sites and transported to the laboratory in sterile containers to prevent microbial contamination. The leaves were thoroughly washed using distilled water to remove dust and debris, air-dried under shade to preserve heat-sensitive phytochemicals, and then ground into a fine powder using an electric mill. For aqueous extraction, 50 g of powdered material were mixed with distilled water and heated at 70 °C for 30 minutes to facilitate the release of bioactive compounds [9]. The mixture was filtered through Whatman No.1 paper, and the filtrate was stored at 4 °C for subsequent nanoparticle synthesis.

### *Phytochemical Screening*

Qualitative phytochemical tests were performed to identify major classes of bioactive compounds present in the extract. Standard methods confirmed the presence of phenolics, flavonoids, tannins, alkaloids, terpenoids, and coumarins, all of which are known to possess strong reducing and antioxidant activities that support nanoparticle formation and stabilization [10].

#### Green Synthesis of ZnONPs

To prepare zinc oxide nanoparticles, the aqueous plant extract was added dropwise to a 1 mM zinc nitrate solution under continuous magnetic stirring. The appearance of a cloudy or milky-white dispersion indicated the initiation of nanoparticle formation. The reaction mixture was incubated in the dark for 24 hours to prevent photoactivation of zinc ions [11]. The resulting suspension was centrifuged at 10,000 rpm for 15 minutes, washed with distilled water three times to remove impurities, and then dried to obtain purified ZnONPs.

#### Characterization of Nanoparticles

The synthesized ZnONPs were characterized using several instrumental techniques: These

included FE-SEM for morphological examination, UV-Vis spectroscopy for assessing the crystalline properties, XRD for structural analysis, and Fourier transform infrared spectroscopy (FTIR).

#### Cell Culture (U87 Human Glioblastoma Cell Line)

U87 cells were cultured in MEM medium supplemented with 10% fetal bovine serum, penicillin, and streptomycin at 37°C in a humidified incubator. The MTT assay was used to estimate cytotoxicity after treating the cells with different concentrations of U-ZnONPs (0–0.01 µg/ml) for 48 hours. MTT solution was then added, followed by DMSO, to dissolve the formazan, and absorbance was measured at 492 nm.

$$\text{Cytotoxicity ratio} = \left[ \frac{(\text{OD}_{\text{control}} - \text{OD}_{\text{sample}})}{\text{OD}_{\text{control}}} \right] \times 100$$

#### Morphological Examination

Cell morphological changes after treatment with U-ZnONPs were observed under an inverted light microscope. Parameters such as cell shrinkage, loss of adherence, and membrane blebbing were recorded as indicators of apoptosis.

#### Statistical Analysis

The results were statistically analyzed based

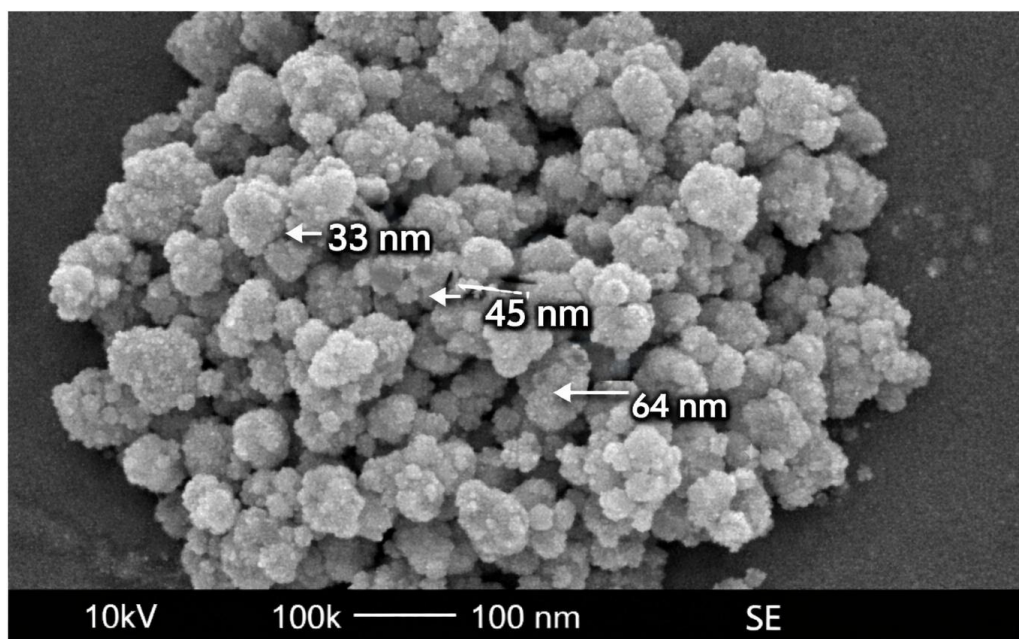


Fig. 1. Field-emission scanning electron microscopy (FE-SEM) to evaluate surface morphology and particle size of (ZnO NPs).

on the completely randomized design, the least significant difference (LSD) test, and the Duncan test for reproducibility between means at the probability level ( $p \leq 0.05$ ).

**Ethical Considerations**

The project was approved as a service evaluation and registered with the Department of Ecology within the department’s science plan. Formal ethical review was waived in accordance with institutional policy, as the project included routine laboratory data without specification. The authors declared no conflict of interest.

**Reporting Standards**

This quality improvement project was prepared in accordance with the SQUIRE 2.0 Excellence

in Quality Improvement Reporting Standards guidelines [17]. The SQUIRE framework is specifically designed to guide the reporting of systematic efforts to improve the quality, safety, and value of healthcare. A complete SQUIRE checklist is available in the supplementary materials accompanying this manuscript.

**RESULTS AND DISCUSSION**

*Detection of active components in U. pilulifera plants*

Table 1 presents the phytochemical screening results of the aqueous extract of *U. pilulifera*, revealing the presence of several bioactive compounds. Positive results were obtained for terpenes, tannins, terpenoids, flavonoids, phenols, coumarins, and alkaloids. In contrast, the

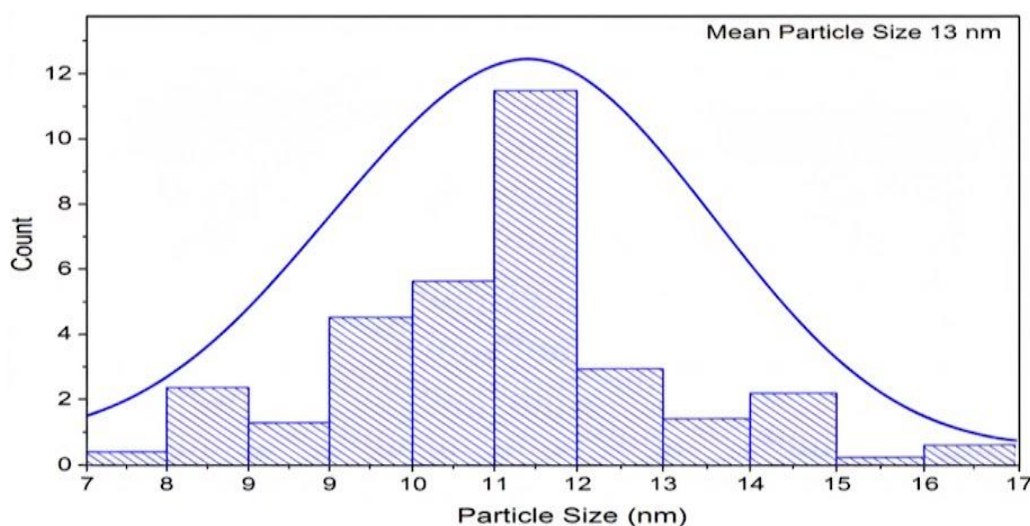


Fig. 2. The synthesized of (ZnO NPs) mean particle size.

Table 1. detection of active components in *U. pilulifera* plants.

N	Tests	Test results	<i>U. pilulifera</i>
1	Glycosides Test		-
2	Terpenes	layer that is reddish-brown	+
3	Trpenoid	Purple and red ring	+
4	Tannins Test	Test for ferric chloride in gelatinous precipitates	+
5	Resins Test	Lead Acetate Test (Color of bluish-green)	+
6	Flavonoids Test	a dark yellow hue Hydroxide of potassium	+
7	Saponins Test	Yellow color sulfuric acid test	+
8	Alkaloids Test	(Dragendroff reagent) Precipitate with an orange hue	+
9	Phenolate Test	Mayer reagent (Turbidity)	+
10	Fuocoumarins Test	Color: bluish-green	+
		The color yellow	+



extract tested negative for glycosides, resins, and saponins.

*Identification of U-ZnON*

*Morphological and Structural Analysis (SEM & XRD)*

The surface topography and grain characteristics of the synthesized nanoparticles were evaluated using Field Emission Scanning Electron Microscopy (FE-SEM). The micrographs (Fig. 1) reveal a predominantly spherical morphology, where primary nanoparticles tend to form clusters or agglomerates. This phenomenon is likely driven by the high surface energy inherent in nanomaterials.

The statistical analysis of the particle size distribution confirms a range between 33 nm and 64 nm, successfully validating the nanometric nature of the product. Such features, including high surface area and dense grain packing, are pivotal for enhancing the physicochemical and catalytic performance of the particles. Interestingly, while the FE-SEM showed larger clusters, the mean particle size was calculated at 12 nm (Fig. 2).

The crystalline integrity of the samples was further examined via X-ray diffraction (XRD). The resulting pattern (Fig. 3) displayed distinct diffraction peaks, with a notably sharp peak attributed to the crystalline phase of the material.

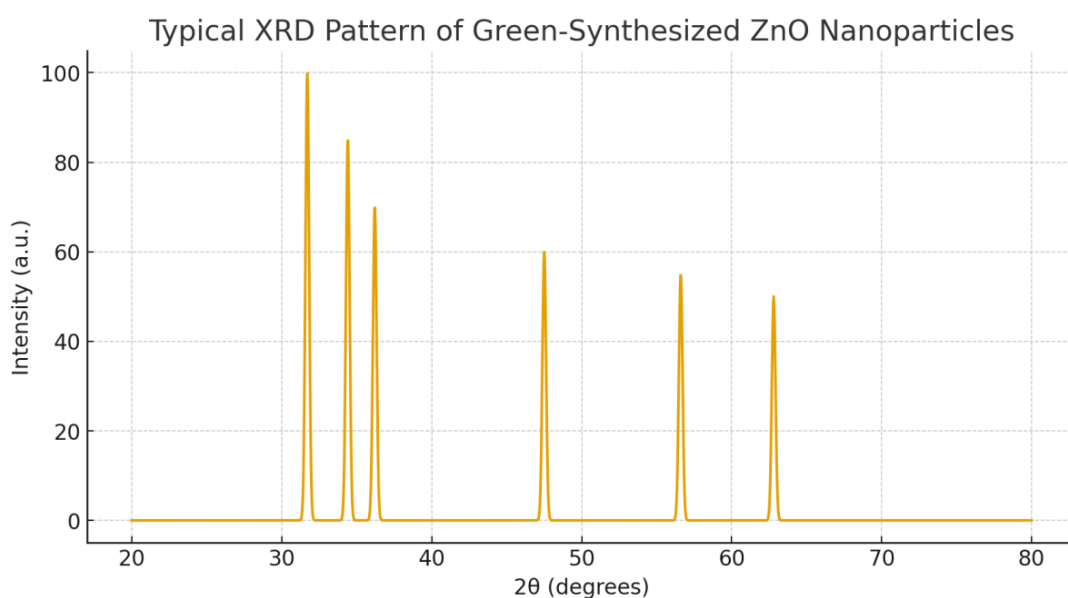


Fig. 3. (XRD) to determine crystalline structure and phase composition of (ZnO NPs).

Table 2. (XRD) of (ZnO NPs) to determine 2θ(Degrees), Miller Indices crystalline structure.

No.	2θ(Degrees)	Miller Indices (hkl)	Crystal Plane
1	31.7°	(100)	Basal Plane
2	34.4°	(2)	Preferred c-axis Plane
3	36.2°	(101)	Major inclined Plane
4	47.5°	(102)	Secondary Plane
5	56.6°	(110)	Lateral Plane
6	62.8°	(103)	High-angle inclined Plane
7	66.3°	(200)	Double reflection Plane
8	68.0°	(112)	High-energy Plane
9	69.1°	(201)	Weak reflection Plane

The presence of these well-defined peaks confirms the transition from an amorphous precursor to a highly crystalline nanostructure, consistent with the standard lattice parameters for such formations.

*Optical Properties (UV-Vis Spectroscopy)*

The optical transformation during the synthesis was monitored using UV-Visible spectroscopy (Fig. 4). The *U. pilulifera* extract (PE) exhibited a characteristic absorption maximum at 280 nm. Upon the formation of nanoparticles, a distinct red shift was observed with the emergence of a new secondary peak at 450 nm. This dual-peak profile retaining the extract’s signature at 280 nm while developing a new band in the 400–450 nm range serves as definitive evidence for the successful

bio-reduction and formation of the nanoparticles of (ZnO NPs).

*FTIR Analysis and Functional Groups Involvement*

To identify the biochemical constituents responsible for the reduction and stabilization of the ZnO NPs, Fourier Transform Infrared (FTIR) spectra were recorded (4000–400  $\text{cm}^{-1}$ ). The crude plant extract displayed vibrational bands at  $\sim 3400 \text{ cm}^{-1}$  (O-H),  $\sim 2920 \text{ cm}^{-1}$  (C-H),  $\sim 1700 \text{ cm}^{-1}$  (C=O), and  $\sim 1050 \text{ cm}^{-1}$  (C-O), indicating a richness in phenols, flavonoids, and proteins. Post-synthesis, these peaks underwent significant intensity reductions and positional shifts, suggesting that these functional groups actively participated in the coordination and reduction of zinc ions.

A definitive “fingerprint” of ZnO formation was

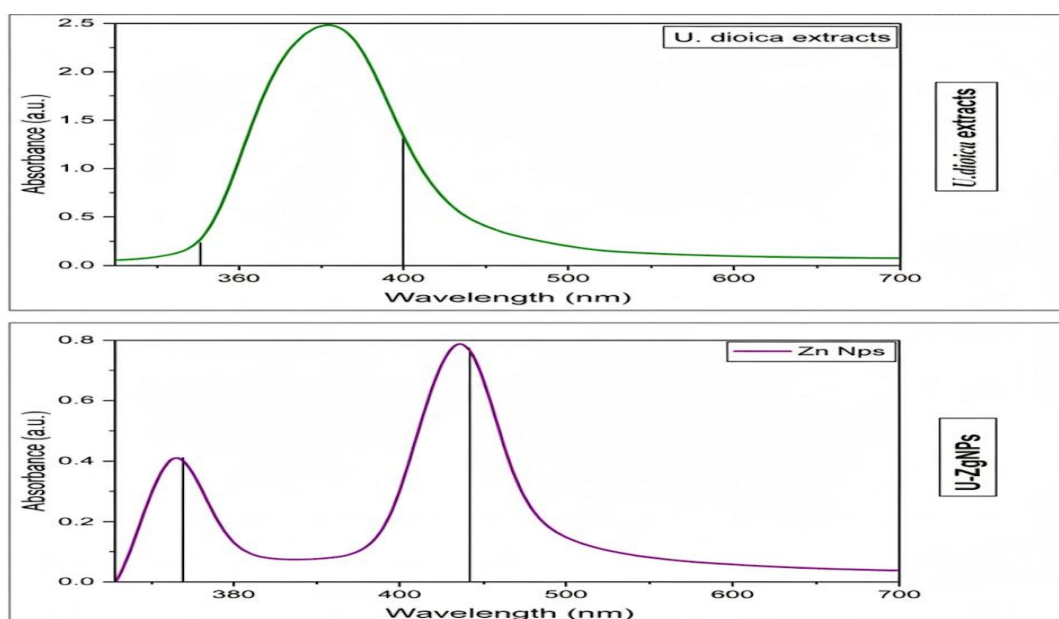


Fig. 4. UV-Visible spectroscopy to confirm nanoparticle formation through characteristic absorption peaks of (ZnO NPs) and (*U. pilulifera* L.) extracts.

Table 3. (FTIR) to identify functional groups responsible for reduction and capping.

Peak Position ( $\text{cm}^{-1}$ )	Functional Group Assignment	Bioactive Component	Role in Synthesis
3400	O-H / N-H stretching	Polyphenols / Proteins	Reduction & Stabilization
1630	C=O / C=C aromatic	Flavonoids / Amides	Capping & Chelation
1060	C-O stretching	Carbohydrates / Esters	Surface Stabilization
450 – 550	Zn-O stretching	ZnO Crystal Lattice	Confirmation of ZnO

identified in the low-frequency region (450–520 cm<sup>-1</sup>). This intense absorption band corresponds to the Zn–O stretching vibrations, confirming the development of a wurtzite-phase crystalline

structure. The absence of this specific band in the raw extract spectrum further validates the chemical conversion of precursors into nano-oxide forms.

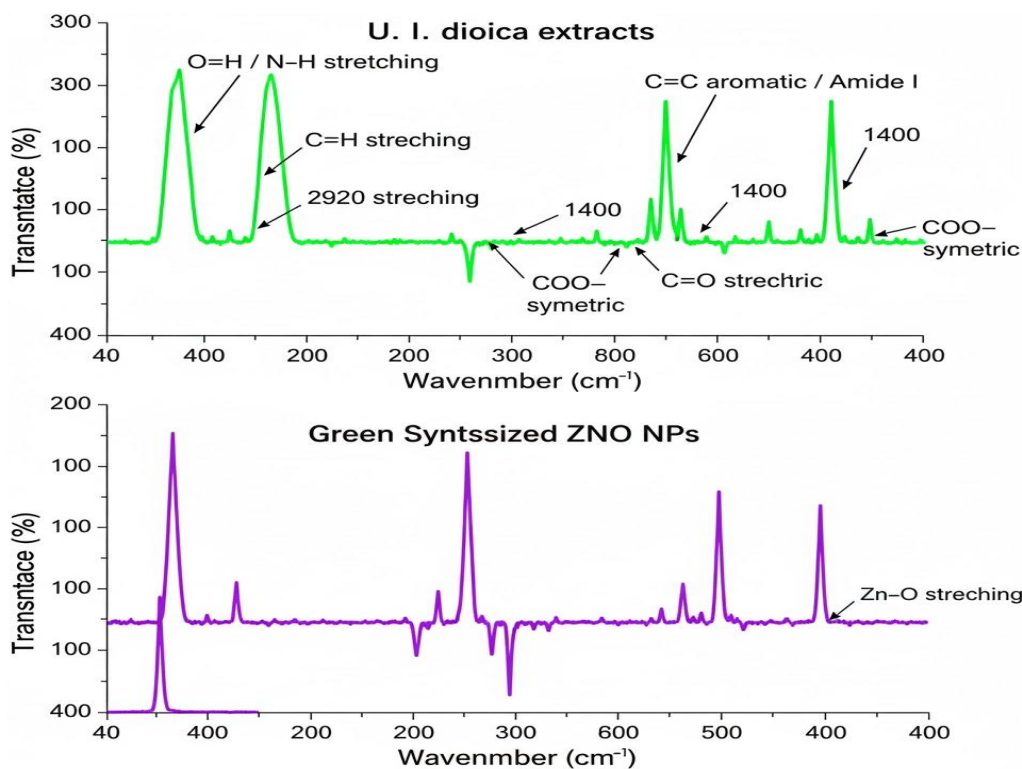


Fig. 5. FTIR Analysis and Functional Groups Involvement of (ZnO NPs) and (*U. pilulifera* L.) extracts.

Table 4. Cytotoxicity of ZnO NPs on U87 cell line.

	ZnO NPs Concentration				
	0	0.00125	0.0025	0.005	0.01
12h	350	332	331	318	309
24h	345	330	328	326	314
36h	362	356	318	333	310
48h	351	341	316	314	311
Mean	352	339.75	323.25	322.75	311
Viability	100	96.51989	91.83239	91.69034	88.35227
SD	7.164728	11.84272	7.36546	8.460693	2.160247
SEM	3.582364	5.92136	3.68273	4.230347	1.080123

$y = -493.1x + 93.501$   
 $R^2 = 0.9141$

IC50=0.08 dilution Factor

**Proposed Mechanism: Biogenic Reduction and Capping**

The spectral data supports a dual-action role for the *U. pilulifera* extract as both a reducing and capping agent. The modification of hydroxyl (O-H) and carbonyl (C=O) signatures implies their direct role in the electron transfer process required to reduce Zn<sup>2+</sup> ions. Moreover, the retention of organic residues (such as amide and C-N bands) on the nanoparticle surface indicates that bioactive macromolecules (proteins and polysaccharides) formed a protective “capping” layer. This naturally occurring coating provides steric stabilization,

which effectively inhibits excessive agglomeration and maintains the long-term structural stability of the nanoparticles.

**Cytotoxicity of ZnO NPs Against U87 Cells**

The cytotoxic activity of ZnO NPs was evaluated using the MTT assay. Results demonstrated a dose-dependent inhibition of U87 cell proliferation. At lower concentrations (0.00125–0.005 ppm), moderate reductions in viability were observed. At the highest concentration (0.01 ppm), cell viability significantly decreased, with survival reduced to ~88.35%. Microscopic examination revealed

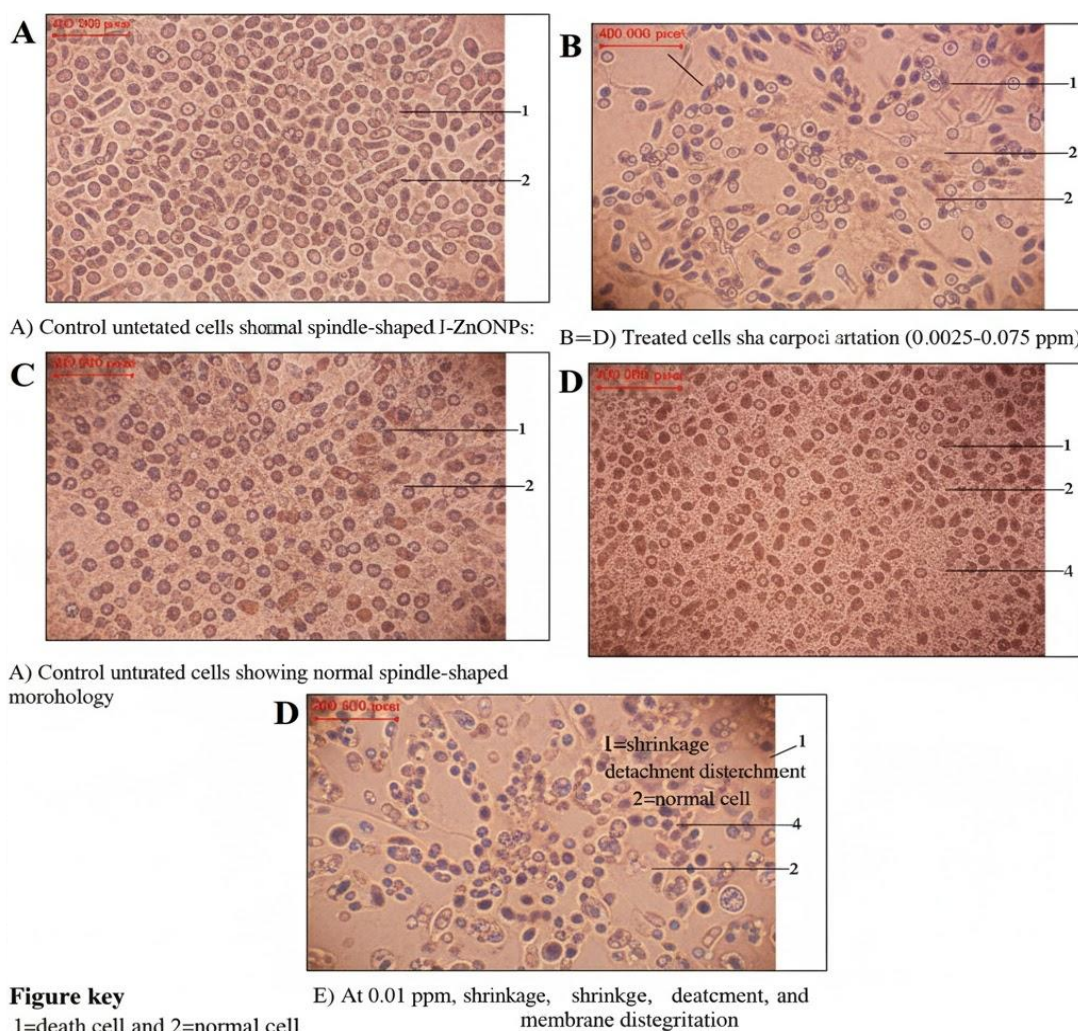


Fig. 6. Morphological changes in U87 glioblastoma cells after treatment with different concentrations of ZnO NPs: (A) Control untreated cells showing normal spindle-shaped morphology. (B–D) Treated cells showing progressive apoptotic features with increasing nanoparticle concentration (0.00125–0.01 ppm). (E) At 0.01 ppm, cells exhibited shrinkage, detachment, and membrane disintegration. Figure key 1=death cell and 2=normal cell.

clear apoptotic changes, including cell shrinkage, rounding, membrane blebbing, and detachment.

#### Morphological Changes in U87 Cells

The results showed that ZnO NPs prepared using *U. pilulifera*(L.) significantly affected U87 brain cancer cells in a concentration- and time-dependent manner (after 48 hours of exposure) at a concentration of (0.00125)ppm it led to a reduction in the size of cancer cells and the appearance of some clusters, which indicates the onset of a cytotoxic effect, possibly by inducing intracellular stress, at a concentration of (0.0025) ppm clear signs of cell killing appeared, which indicates that the toxic effect has reached a level at which actual cell death occurs, The highest kill was at (0.01)ppm a mean 311 error rate 2.16025 with significant differences 1.08012. voids appeared in the place of dead cells, which indicates a massive destruction of cancer cells in this area, as can be seen in Tables 4 and 5 and Fig. 6.

The results of this study indicate that nettle extract (*U. pilulifera* L.) has clear antitumor activity, particularly against glioma brain cancer cells. The data showed a significant decrease in cancer cell viability in a concentration- and time-dependent manner, consistent with previous research on the cytotoxic effects of plant compounds extracted from nettle [26]. This effect is likely related to estrogen receptor pathways, as other studies have shown [27]. These results are also consistent with the findings of Kriegl *et al.* [28], who indicated that the bioactive components of nettle can stimulate apoptosis signaling pathways and inhibit cancer cell division by affecting chromatin receptors, leading to accelerated cell death. Previous studies, consistent with the results of the current research, have shown that the increase in apoptosis rate is directly proportional to both

time and dose. This suggests that nettle extract not only inhibits cell division but also effectively activates apoptosis mechanisms. The results also showed that the extract's toxic effect on normal human fibroblasts was limited (<10%), indicating high selectivity toward cancer cells, a key factor in modern therapeutic applications. This selective toxicity is consistent with other reports that have confirmed the safety of nettle extracts on healthy cells [29]. Overall, the study concluded that the green synthesis of ZnO NPs using nettle extract contributes to inducing apoptosis in cancer cells with very little effect on normal cells. The results recommend expanding future studies to explore the effectiveness of these particles against other types of cancerous tumors, to evaluate their potential as a promising therapeutic agent in the field of nanomedicine.

#### Limitations

Despite the promising anticancer activity of ZnO NPs synthesized using nettle, this study has several limitations. First, all in vitro experiments were performed on a single cancer cell lineage (U87), limiting the extrapolation of results to in vivo conditions. The molecular mechanisms of cytotoxicity were not fully elucidated, as no apoptosis markers, reactive oxygen species (ROS) levels, or gene expression analyses were performed. Furthermore, important nanoparticle properties, such as zeta potential, DLS, and long-term stability, were not assessed. The study also did not compare the nanoparticles to standard chemotherapeutic agents. The phytochemicals responsible for the observed activity were not quantified using advanced analytical techniques. Therefore, further in vivo studies, mechanistic investigations, and broader cytotoxicity assays are needed to verify the therapeutic potential of ZnO

Table 5. Summary of key morphological observations of cells under control conditions and after treatment.

Panel	Condition	Key Morphological Observations
A	Control	Cells exhibit normal, spindle-shaped morphology and strong adherence to the culture plate (labeled as normal cells, '2').
B-D	Treated	As the concentration of U-ZnONPs increases (from low to moderate doses), cells progressively develop apoptotic features, including initial shrinkage and cell rounding.
E	Highest Dose	At the highest concentration (e.g., 0.01 ppm), cells show severe cytotoxicity: extensive cellular shrinkage, detachment from the substrate, and clear signs of membrane disintegration/lysis (labeled as death cells, '1').

NPs.

## CONCLUSION

The current study demonstrated anticancer activity against tested cancer cells. Cell proliferation was inhibited and apoptosis was accelerated. Microscope images showed that the effect targeted cancer cells but not healthy cells. The results showed that the lethal effect of the nanomaterials and extract increased with increasing concentration and time. These findings suggest that nettle extract could be a promising natural anticancer agent. Future research should focus on isolating the active phytochemicals, elucidating the molecular mechanisms underlying its anticancer effects, and conducting in vivo studies to verify its efficacy and safety in potential therapeutic applications.

## ACKNOWLEDGMENTS

Many thanks and gratitude to the University of Kufa, College of Science, Department of Ecology for the scientific support, laboratories and consultations they provided.

## CONFLICT OF INTEREST

The authors declare that there is no conflict of interests regarding the publication of this manuscript.

## REFERENCES

1. Ali AT, Guda MA, Oraibi AI, Salih IK, Shather AH, Abd Ali AT, et al. Fe<sub>3</sub>O<sub>4</sub> supported [Cu(ii)(met)(pro-H)<sub>2</sub>] complex as a novel nanomagnetic catalytic system for room temperature C–O coupling reactions. *RSC Advances*. 2023;13(32):22538-22548.
2. Ali M, Othman M, Guda M, Abojassim A, Almayahi B. Effect of Climate Characteristics in the Scientific Levels of Students: An Applied Study on the City of Najaf. *Journal of Physics: Conference Series*. 2020;1530(1):012142.
3. Guda MA. Retraction: Response of antioxidant in some plants to iron oxide nanoparticles. *AIP Conference Proceedings: AIP Publishing*; 2023. p. 040144.
4. Guda MA, Mutlag NH, Tsear AA. The use of *Atriplex nummularia* plant as the hyperaccumulators of silver. *AIP Conference Proceedings: AIP Publishing*; 2020. p. 020041.
5. Husayn DM, Guda MA. Response of some wild plants in antioxidant enzymes by zinc oxide nanoparticles. *AIP Conference Proceedings: AIP Publishing*; 2023. p. 090049.
6. Husayn DM, Guda MA. Effect of zinc oxide nanoparticles on biomarkers of chlorophyll and carotene in some wild plants. *AIP Conference Proceedings: AIP Publishing*; 2023. p. 090035.
7. Mutlag NH, Guda MA, Hussein ML, Hassan HN. Assessment of *Bombax ceiba* Leaves Extract and *Pleurotus ostreatus* Fungus Filtrate on treatment of some Isolated Dermatophytic Fungi. *Journal of Physics: Conference Series*. 2019;1294(7):072022.
8. Effect Of Two Tomatoes (*Lycopersicon Esculentum* Mill.) Seedling Conditioning with Saline Water on Vegetative Growth. *Basrah Journal of Agricultural Sciences*. 2008;21(2):45-60.
9. Rahy AY, Guda MA. Evaluation of The Inhibitory Activity of Aqueous and Alcoholic (*Punica granatum*) Pomegranate Peel Extract on Some Bacterial species Isolated from Patients' beds at Al-Refai Teaching Hospital. *International Journal of Advancement in Life Sciences Research*. 2025;08(02):186-193.
10. Al-Khafaji BAH, Guda MA, Al-Edhari AH, Altamimi AJT. Taxonomic Study for the Genus *Bupleurum* L. (Apiaceae) in Iraq using chloroplast gene RPL16. *Indian Journal of Public Health Research and Development*. 2019;10(1):713.
11. Guda MA, Nasir AS, Younus AS, Altamimi AJT. Antioxidant Enzyme Responses of *Juncus Aschers.* (Et Buch.) Adams to Some of Environmental Stresses and use it as Indicators. *Indian Journal of Public Health Research and Development*. 2018;9(12):1102.
12. Guda MA, Obaid JK, Alduhaidahawi Fj, Alkurdi HJA, alkareemaw HGL, Salih HM, et al. The role of street and park trees to CO<sub>2</sub> removal and improving air quality and climate in urban areas in Najaf (Iraq) Type the title of your paper here. *IOP Conference Series: Materials Science and Engineering*. 2020;870(1):012087.
13. Al-Sharifi S, Al-Bakri S, Al-Bayati S. Evaluation of Eutrophication Levels in Al-Najaf Al-Ashraf Lake, Iraq (Biological and Chemical study). *Engineering and Technology Journal*. 2020;38(10A):1531-1538.
14. Bailly C. Review: Natural products isolated from *Portulaca oleracea* (purslane, Ma-Chi-Xian): Focus on oleraciamides and oleracones. *Nusantara Bioscience*. 2021;13(2).
15. Guda M, Hakeem J, Alabassi M, Almayahi B. Effects of Environmental Stress on Nutrients of *Typha domingensis* Pers. Plant in Najaf, Iraq. *Annual Research and Review in Biology*. 2017;19(3):1-6.
16. alkareemaw HGL, Guda MA, Alabassi MM, taheer Mae, Altamimi AJT, Alhadrawi HAN. Use of wild plant species as indicator of some heavy metals in the soil of General Company for tire industry in Najaf Governorate. *IOP Conference Series: Materials Science and Engineering*. 2020;870:012099.
17. Ogrinc G, Davies L, Goodman D, Batalden P, Davidoff F, Stevens D. SQUIRE 2.0 (Standards for Quality Improvement Reporting Excellence): revised publication guidelines from a detailed consensus process. *BMJ Quality and Safety*. 2015;25(12):986-992.
18. Muthik A. Guda EAa-RAS. Response Of A Medicinal Plant *Peganum Harmala* To Iron Oxide Nanoparticles F3O4(Nps). *Journal of Pharmaceutical Negative Results*. 2022:990-999.
19. Al-Shammeryi WHM. Effects of seed coating with (titanium dioxide and selenium) nanoparticles on fenugreek (*Trigonella foenum graecum* L.) plant growth and antioxidant activity. *Advancements in Life Sciences*. 2024;11(4):810.
20. Abed EY, Kadhim HF, Guda MA. The Effects of Climate Change on Public Health. *Contemporary Research Analysis Journal*. 2025;02(08).
21. Hamood SAA-M, Khaleel DA, Guda MA. Harnessing Artificial Intelligence to Revolutionize Public Health: Innovations in Prevention, Monitoring, and Policy Decision-Making.

- Contemporary Research Analysis Journal. 2025;02(08).
22. Johnson-Ajinwo OR, Richardson A, Li W-W. Cytotoxic effects of stem bark extracts and pure compounds from *Margaritaria discoidea* on human ovarian cancer cell lines. *Phytomedicine*. 2015;22(1):1-4.
  23. Tak N. Type-1 recurrent intuitionistic fuzzy functions for forecasting. *Expert Systems with Applications*. 2020;140:112913.
  24. Jafari Z, Samani SA, Jafari M. Insights into the bioactive compounds and physico-chemical characteristics of the extracted oils from *Urtica dioica* and *Urtica pilulifera*. *SN Applied Sciences*. 2020;2(3).
  25. Francišković M, Gonzalez-Pérez R, Orčić D, Sánchez de Medina F, Martínez-Augustin O, Svirčev E, et al. Chemical Composition and Immuno-Modulatory Effects of *Urtica dioica* L. (Stinging Nettle) Extracts. *Phytother Res*. 2017;31(8):1183-1191.
  26. Abi Sleiman M, Younes M, Hajj R, Salameh T, Abi Rached S, Abi Younes R, et al. *Urtica dioica*: Anticancer Properties and Other Systemic Health Benefits from In Vitro to Clinical Trials. *Int J Mol Sci*. 2024;25(13):7501.
  27. Eren A, Varol M, Unal R, Altan F. Exploring *Urtica dioica* L. as a Promising Alternative Therapy for Obesity-Related Breast Cancer: Insights from Molecular Mechanisms and Bioinformatic Analysis. *Plant Foods Hum Nutr*. 2025;80(2).
  28. Dakhli N, López-Jiménez A, Cárdenas C, Hraoui M, Dhaouafi J, Bernal M, et al. *Urtica dioica* Aqueous Leaf Extract: Chemical Composition and In Vitro Evaluation of Biological Activities. *Int J Mol Sci*. 2025;26(3):1220.
  29. Tavanaei F, Mohammadgholi A, Asghari Moghaddam N. *Urtica dioica* Mediates Zinc-Copper Doped Nanoparticles as Potent Anticancer Agents against Human Breast Cancer MDA-MB-231 Cell Line. *Advanced Biomedical Research*. 2025;14(1).